magnetochemistry

MDPI

Review

The Origins and the Current Applications of Microfluidics-Based Magnetic Cell Separation Technologies

Ozgun Civelekoglu [1], A. Bruno Frazier [1,2,*] and A. Fatih Sarioglu [1,2,3]

[1] School of Electrical and Computer Engineering, Georgia Institute of Technology, Atlanta, GA 30332, USA; ocivelekoglu@gatech.edu (O.C.); sarioglu@gatech.edu (A.F.S.)
[2] Institute for Electronics and Nanotechnology, Georgia Institute of Technology, Atlanta, GA 30332, USA
[3] Parker H. Petit Institute for Bioengineering and Bioscience, Georgia Institute of Technology, Atlanta, GA 30332, USA
* Correspondence: bruno.frazier@ece.gatech.edu

Abstract: The magnetic separation of cells based on certain traits has a wide range of applications in microbiology, immunology, oncology, and hematology. Compared to bulk separation, performing magnetophoresis at micro scale presents advantages such as precise control of the environment, larger magnetic gradients in miniaturized dimensions, operational simplicity, system portability, high-throughput analysis, and lower costs. Since the first integration of magnetophoresis and microfluidics, many different approaches have been proposed to magnetically separate cells from suspensions at the micro scale. This review paper aims to provide an overview of the origins of microfluidic devices for magnetic cell separation and the recent technologies and applications grouped by the targeted cell types. For each application, exemplary experimental methods and results are discussed.

Keywords: microfluidics; magnetophoresis; cell separation

Citation: Civelekoglu, O.; Frazier, A.B.; Sarioglu, A.F. The Origins and the Current Applications of Microfluidics-Based Magnetic Cell Separation Technologies. *Magnetochemistry* **2022**, *8*, 10. https://doi.org/10.3390/magnetochemistry8010010

Academic Editor: Marie Frenea-Robin

Received: 28 November 2021
Accepted: 4 January 2022
Published: 11 January 2022

1. Introduction

Magnetic cell separation, namely magnetophoresis, refers to the selective isolation of certain cell populations from a more complex, heterogeneous suspension with the aid of an external magnetic field targeting the magnetically susceptible components within the sample. For biological samples, these targeted components are often the deoxygenated hemoglobin present in the red blood cells (RBCs), which shows paramagnetic properties [1], diamagnetic behavior of white blood cells (WBCs) in blood plasma [1], or superparamagnetic nano-/micro-particles selectively tagging desired cell populations [2–4]. To supply a magnetic gradient to the system, permanent magnets, electromagnetic coils/wires or a combination of these two approaches can be applied. Furthermore, magnetophoresis can be tuned for positive and negative isolation. Positive isolation refers to isolating the cellular population of interest by using a magnetic field gradient to create a magnetic force in the direction of the magnetic field gradient. Subsequently, the magnetic force is applied to targeted cells to attract them away from the rest of the sample. Negative enrichment, on the other hand, focuses on eliminating every cell other than the population of interest by magnetically depleting them, leaving the non-magnetic desired cells purified and untouched. While positive isolation offers high-purity yields (>99%) compared to a negative enrichment, which may suffer from unintentional collection of non-target cells, the negative enrichment mode allows separation without stressing the target cells and the possibility of purifying cell populations without a known biomarker [5].

Although magnetic cell separation is widely practiced for research, it is also actively used in clinical environments [4], from diagnostic microbiology [6], collection of stem cells [7,8] and purifying manufactured CAR-T cells [9,10] to selection of motile sperms [11,12]. The main advantages of magnetophoresis in these applications over

fluorescence-based separations technology, where the cell population of interest are tagged with fluorescent labels and selectively refined into a collection vessel [13], was their straightforward protocols and rapid processing with high throughput.

Magnetic separation in the macro domain has long been established for isolating cells populations such as RBCs [14–17], WBCs [18–20] and rosette-forming cells [21], as well as to separate ultra-fine particles [22]. These technologies all used a high-gradient magnetic field to compensate for the miniscule magnetic susceptibility in their respective biological samples [23]. Since then, significant effort has been dedicated to miniaturizing magnetic separation in order to achieve precise control in the micro-environment [24], geometrical advantages of miniaturization [25], microfabrication of devices in batches [26], low cost [27], and superior assay portability [28]. Furthermore, microfluidic devices offer capability of integration with other mechanisms to increase performance [29,30], high-throughput measurements [31,32], and rapid detection rates [33–35], making them ideal for clinical applications at the point of care [36,37].

This paper reviews the origins of the magnetic separation demonstrated in microfluidic platforms and the current literature grouped by the types of cells being separated. The next section (Section 2) provides an overview of how microfluidics and magnetic sorting were brought together. Section 3 presents the current platforms developed to separate blood cells as well as their specific subpopulations. The isolation of tumor cells in general microfluidic platforms was recently reviewed by Farahinia et al. [38], and the magnetic separation techniques for circulating tumor cells were briefly mentioned by Surendran et al. [39]. Compared to these recent reviews, we discuss the different magnetic sorting approaches to isolate cancer cells in detail in Section 4. In Section 5, we review the technologies enabling a multiplexed sorting in the magnetic domain, as well as the cases where magnetophoresis was used to uncover population-level dynamics instead of a binary-level separation.

2. The Origins of Microfluidic Magnetophoresis

Microfluidics and magnetic sorting were integrated together to overcome the relatively small magnetic flux gradients possible in macro-scale magnetic separators. Using the advantages of micromanipulation and miniaturization, magnetic sorting was applied to the separation of droplets [40], polystyrene beads [40,41], magnetic beads [41,42], and agglomerates [41]. Berger et al. [43] demonstrated some progress in cell sorting with magnetophoresis with a microfabricated device containing microwires made out of a cobalt–chrome–tantalum alloy; however, the group failed to fully fractionate the cell populations. They highlighted the challenges of optimizing the hydrodynamic forces, preventing the entrapment of beads under magnetic field and the importance of surface passivation. One of the first implementations of a cell sorting in microfluidics-based magnetophoretic was created to segregate RBCs and WBCs using their native magnetic properties. Initially, Han et al. [44] developed a theoretical model RBC movement under laminar flow and the magnetic forces focused by a ferromagnetic wire, which was made out of nickel, under an external magnetic field. Using this model, Han et al. [44,45] also developed a magnetophoretic cell separator with one inlet and three outlets to separate RBCs from whole blood (Figure 1). By focusing an external magnetic field into a microfluidic channel using a micropatterned ferromagnetic wire, they achieved 92% efficiency in separation of RBCs from whole blood with this microfluidic device.

By altering the direction of the external magnetic field, Han et al. demonstrated both diamagnetic [46] and paramagnetic [47,48] modes for the separation. The group showed that when the external field was normal to the microfluidic plane, the ferromagnetic wire deformed the magnetic field in its vicinity and created a high magnetic gradient forcing paramagnetic particles towards the edges of the microfluidic channel (Figure 2a). In contrast, when the magnetic field was applied perpendicular to the ferromagnetic wire within the plane of the microfluidic features, the magnetic flux was concentrated towards the wire, generating an increasing magnetic gradient towards the center of the microfluidic channel (Figure 2b). In diamagnetic mode, Han et al. achieved an efficiency of 89.7% for RBCs and

72.7% for WBCs [46]. These numbers were improved in their paramagnetic mode with separation efficiencies of 93.5% and 97.4% for RBCs and WBCs, respectively [47].

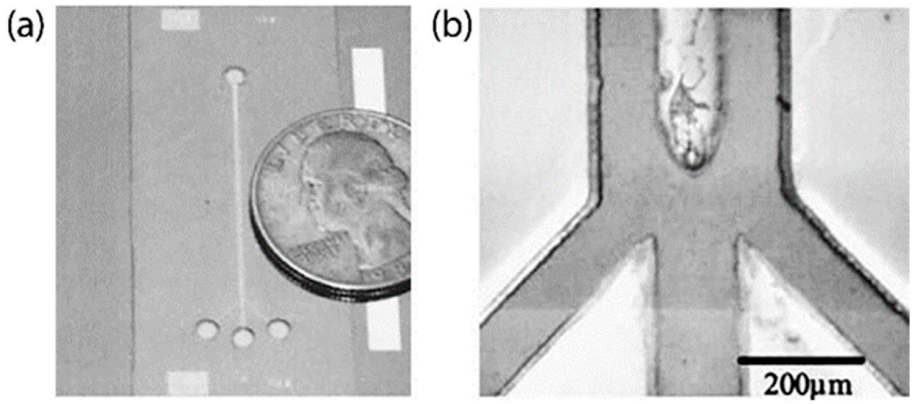

Figure 1. Initial implementation of magnetophoretic separator in a microfluidic platform. (**a**) Top view of the device. (**b**) Microscopic view. Reprinted from [44] with the permission of AIP Publishing, copyright 2004.

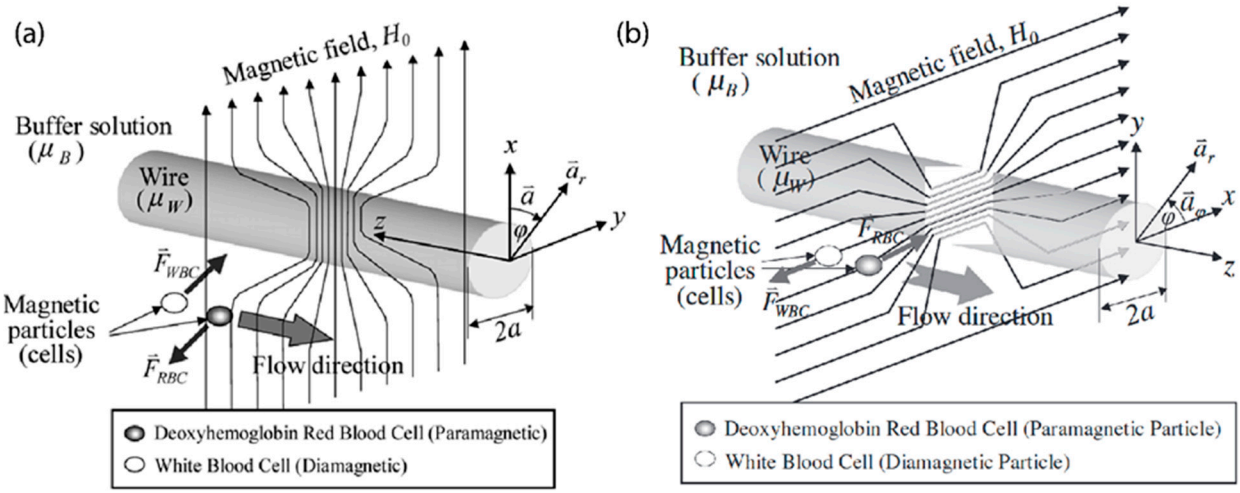

Figure 2. Operational modes for the microfluidic sorter. (**a**) Diamagnetic mode. Copyright 2005 IEEE. Reproduced with permission from [46]. (**b**) Paramagnetic mode for operation. Reproduced with permission [48]. Copyright 2006 IET.

Alternative to using the native magnetic properties of blood cells, Inglis et al. [49] used paramagnetic nanoparticles that are used in the bulk separation. They specifically used nanobeads conjugated with CD45, a common leukocyte surface marker, to amplify the magnetic force on WBCs. The ferromagnetic strips with an angle shift with respect to the direction of fluidic flow were micropatterned out of Nickel on the floor of the microfluidic device. These nickel features allowed them to direct tagged WBCs away from RBCs under a magnetic field as low as 0.08 T [49] compared to the 0.6 T in the first magnetic-activated cell sorting system [50] or 0.2 T used by Han et al. [46,47].

Furdui et al. [51] developed a microfluidic device with capture beds to isolate T-cells from blood samples using a simple NdFeB permanent magnet and CD3-conjugated magnetic beads without any additional patterning of paramagnetic features. The magnetic particles were first deposited into the capture beds, then 2 µL of blood sample was introduced into the device to selectively grab CD3+ T-cells under continuous flow. Under the optimized flow rate of 0.25 µL/min, a capture efficiency of 42% was achieved.

The application of magnetic separation outside of WBC versus RBC field was demonstrated for label-free negative enrichment of breast cancer cells circulating in the blood

stream. In this study, Han et al. [52] applied their paramagnetic separator with Nickel wire as an enrichment stage which was then coupled with a micro-scale electrical impedance spectroscopy (μ-EIS) [53] for detection. Using the paramagnetic properties of deoxygenated RBCs, WBCs and the breast cancer cells spiked in blood were separated from the RBCs, and their subsequent μ-EIS measurements not only distinguished the malignant cells from the healthy population, but also detected different pathological stages of the cancer cells [52].

3. Advances in Magnetic Separation of Blood Cells by Cell Type

3.1. RBC and WBC Separation

In recent years, efforts have been made to test different magnetophoretic systems to separate RBCs and WBCs from whole blood, as summarized in Table 1. A microfluidic blood cell separator was developed by Shiriny et al. [54] with magnetic elements stacked in a Halbach array format, a spatially rotating arrangement of permanent magnets that creates a strong and near-zero weak magnetic field side on two opposing faces of the arrangement [55]. Although they reported slow flow rates up to 15 μL/h, the Halbach structure allowed a straightforward scaling while keeping the separation efficiency at its peak. Another work demonstrated self-assembling micromagnets enclosed in a polymer layer to deplete WBCs [56]. Unlike other works where the gradients are amplified by spatial patterning of ferromagnetic materials, this system accomplished fine tuning of the local magnetic gradients with the arrangement of the micromagnets. However, the authors also reported that an external magnetic field was necessary to improve the efficiency beyond 85%, especially for flow rates equal to or greater than 0.5 mL/h.

Separation of blood cells in microfluidics transitioned into clinical applications. This trend was reviewed in depth both in terms of the analytes in clinical and forensic field [57] and in terms of technical aspects [58]. One of these applications where magnetophoresis was employed to separate blood cells was for non-invasive prenatal diagnostics. Cascading a commercial positive enrichment with a magnetophoretic chip, Byeon et al. [59] developed a platform that isolated the nucleated red blood cells from maternal blood for further fluorescent and genetic testing. In this work, magnetic micropatterns were fabricated to eliminate magnetically labeled WBCs from the initially enriched population of nucleated blood cells (Figure 3). The system worked remarkably well to enrich the rare, nucleated RBCs, yet the system had to resort to a pre-concentration of the blood sample to be effective.

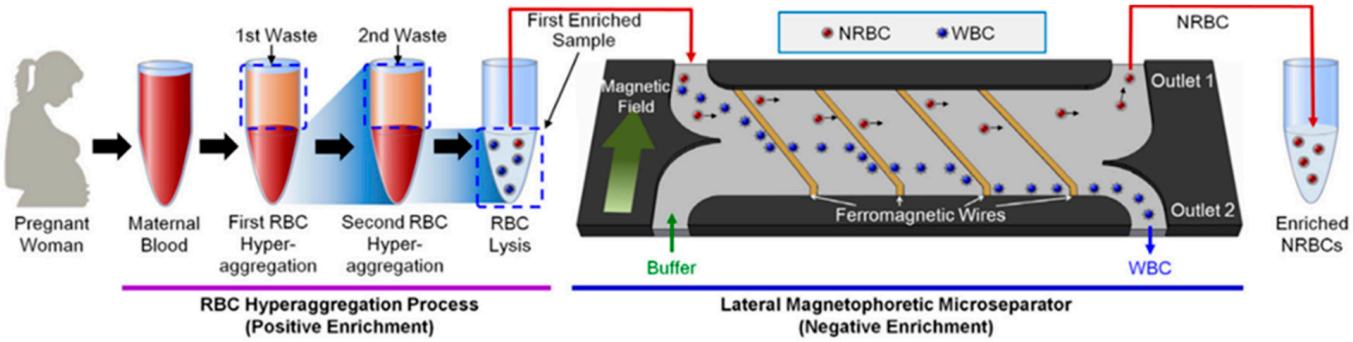

Figure 3. Magnetophoretic platform for prenatal diagnostic testing. Nucleated red blood cells in the maternal blood sample were isolated using a magnetophoretic microseparator for further testing. Reproduced with permission [59]. Copyright 2015 Springer Nature.

Microfluidic magnetophoresis was employed for the detection and removal of malaria-infected red blood cells (iRBCs). This application stems from the increased paramagnetism observed in iRBCs since the parasite catabolizes the heme in hemoglobin into a highly concentrated crystal called hemozoin [60]. Kim et al. [61] proposed a dialysis-like microfluidic system (Figure 4a) to continuously eliminate iRBCs from the blood stream by patterning magnetic wires in a periodic grid, and they demonstrated the feasibility of such approach by computational analysis. Later, the same group presented a prototype of their

system (Figure 4b) that achieved a removal rate of 27% in a single run at a processing rate of 77 µL/min [62]. The authors also discussed that once scaled up, the platform could reduce the parasitemia in patients to 1% after processing 3 units of blood in about 65 min. However, the data in the work was limited to samples with cells that were analogous to malaria-infested cells rather than demonstrating data from actual patient samples.

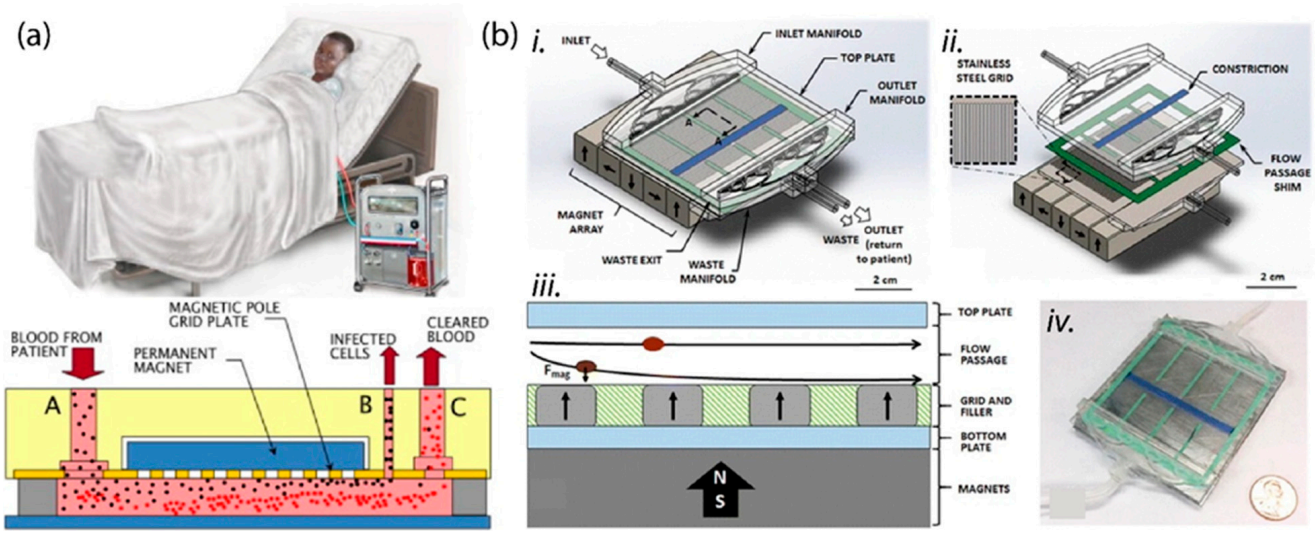

Figure 4. Magnetophoretic removal of malaria-infected red blood cells. (**a**) Conceptual design. Reproduced with permission [61]. Copyright 2012 Elsevier. (**b**) High-throughput microfluidic platform to separate malaria-infected RBCs. Reproduced with permission [62]. Copyright 2017 Springer Nature.

3.2. Separation of Specific Hematological Cells

3.2.1. CD4+ T-Cell Enrichment

Magnetic beads can be conjugated with antibodies to specifically amplify the magnetic susceptibility of a target cell population. Glynn et al. [63] used antibody-conjugated magnetic beads to capture CD4+ (biomarker for helper T-cells [64]) cells and estimate their concentration in an instrument-free microfluidic chip for AIDS diagnosis and periodic prognosis in resource-poor regions. In this work, an immunomagnetically labeled sample was loaded into the device with a simple finger press on a fluid reservoir, which allowed the magnetically labeled cells to be pulled by the external magnetic field and accumulate in a stagnant flow region for quantification (Figure 5). With this platform, the authors achieved processing of a 4-µL blood sample in a remarkable 45 s. Another work [65] used magnetophoretic separation to enrich CD4+ cells and integrated it with a DNA-induced bead aggregation for quantification. Their approach consisted of two consecutive enrichment stages, with the first step depleting the CD14+ (biomarker for myelomonocytes [64]) cells and the second step accumulating CD4+ cells. The concentrated T-cell population was lysed to reveal genetic content and its mass was measured by the aggregation of DNA targeting silica coated magnetic beads. Although the measurement of genetic material, especially the viral load, is desirable for better clinical decisions [66], this work still relied on the phenotype of T-cells. It would be quite interesting to see this technique applied for viral load measurements.

3.2.2. Depletion of CD19+ B-Cells in T-Cell Manufacturing

Microfluidics facilitated the precise isolation of rare cells present in blood. In CAR T-cell manufacturing, any contaminant cell, such as leukemic B-cells, must be eliminated prior to administration to prevent the failure of the therapy. To ensure purity of the CAR T-cells during quality control, Wang et al. [67] developed an immunomagnetic ranking system to purge contaminant CD19+ B-cells (Figure 6). By patterning ferromagnetic features with an

increasing thickness throughout the device, they created capture regions sensitive to the varying number of magnetic nanoparticles present on the cells. Passing a cell population with contaminant cells through their microfluidic chip, 99.985% capture efficiency and above 90% recovery of T-cells was achieved [67]. The authors claimed they exceeded the efficiency of the leading commercial magnetic-activated cell sorting (MACS) kits (93.59%).

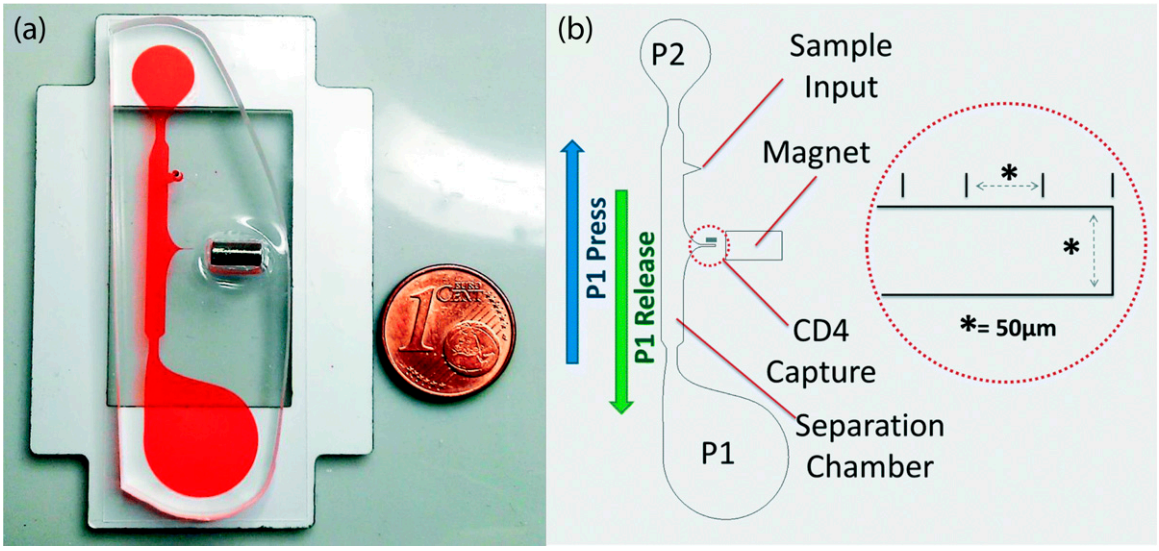

Figure 5. Finger-press-operated magnetophoretic cell separator for CD4+ isolation. (**a**) Image of the microfluidic chip with an embedded permanent magnet. (**b**) Schematic of the components. Reproduced with permission [63]. Copyright 2014 RSC.

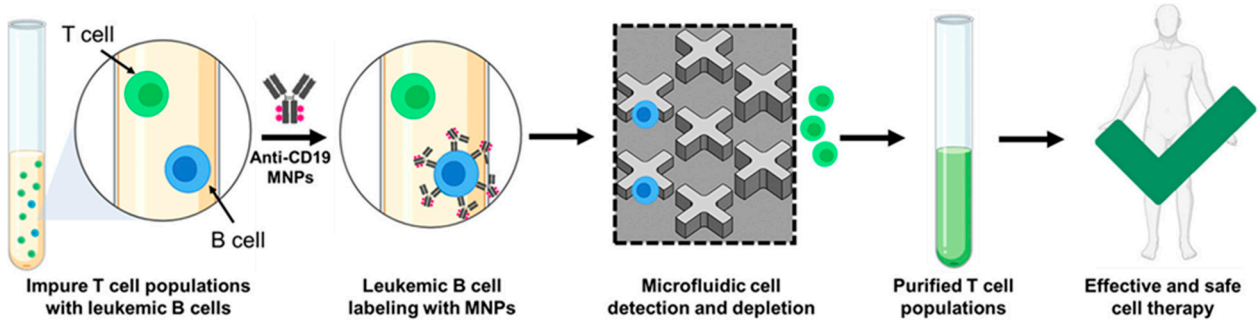

Figure 6. Immunomagnetic purification of CAR T-cells from contaminant leukemic B-cells. Reproduced with permission [67]. Copyright 2021 ACS.

3.2.3. Hematopoietic Stem Cells

Isolation of hematopoietic stem cells (HSCs), which are the precursors of all types of blood cells, from peripheral blood was demonstrated using magnetophoresis. Schneider et al. [68] proposed a microchip sandwiched under a magnetic dipole to sort the HSCs by targeting their CD34 expression (common biomarker for HSCs and endothelium [64]) with nanobeads. However, this study was limited to demonstrating the sorting in the absence of RBCs and had a low yield (47.6%) due to low expression levels of CD34 in the target population. In another technology focusing on the HSCs, the target cells were immunomagnetically labeled with CD133 (a stem cell biomarker [64]) conjugated superparamagnetic microbeads. The labeled HSCs were then separated from whole blood with an efficiency of 96% directly from whole blood [69]. Considering the heterogeneous nature of whole blood, the platform also demonstrated great purity, only 45–60 RBCs remaining after processing 1 mL of blood.

Table 1. Summary of the recent magnetophoretic separation of blood cells.

Authors	Purpose	Target Biomarker	Key Feature	Metrics	Throughput
Shiriny et al. (2020) [54]	WBC/RBC separation	Hemoglobin	Straightforward scaling, minimal external magnetic effects by Halbach array	100% efficiency	15 µL/h
Descamps et al. (2021) [56]	WBC depletion	CD45, CD15	Self-assembling magnets, fine control in localization	85–100% efficiency	0.5 mL/h
Byeon et al. (2015) [59]	WBC depletion	CD45, CD66b	Magnetic amplification by ferromagnetic wire, allows non-invasive diagnostics, but the sample must be pre-concentrated	93.98% efficiency	0.5 mL/h
Blue Martin et al. (2017) [62]	Depletion of malaria-infected cells	Hemozoin (catabolized hemoglobin)	Dialysis-like treatment for malaria, straightforward scaling	27% efficiency	77 µL/min
Glynn et al. (2014) [63]	CD4+ cell enumeration	CD4	Instrument-free operation, simple read-out	93% efficiency	4 µL in 45 s
Q. Liu et al. (2015) [65]	CD4+ cell enumeration	CD14, CD4, DNA	Genetic material-based	95% efficiency	100 µL/min
Wang et al. (2021) [67]	B-cell depletion in cell manufacturing	CD19	Extreme sensitivity, great performance against commercial methods	99.985% efficiency (90% T-cell recovery)	4 mL/h
Schneider et al. (2009) [68]	Fractionation of CD34+ cells	CD34	Differentiation based on degree of magnetization	47.6% efficiency	3 mL/h
Plouffe et al. (2012) [69]	Enrichment of hematopoietic and endothelial progenitor cells	CD133	Processing directly whole blood, high efficiency for rare cell populations	96% efficiency	120 µL/min

4. Advances in the Magnetic Separation of Cancer Cells

Circulating tumor cells (CTCs), which are the tumor cell populations detached from the original site and entered the blood circulation, can provide precious information about the cancer biology in a minimally invasive procedure. Consequently, the separation of CTCs from blood has gained significant attention. In this section, we will discuss the recent works which have demonstrated the isolation of CTCs via magnetophoresis in a microfluidic platform. For simplicity, the literature will be grouped into positive and negative separation methods. In comparison, the positive separation yields superior purity, but lower capture rates due to use of a biomarker and less than perfect efficiency. The negative separation, on the other hand, often presents higher CTC capture rates as the CTCs flow untouched, but the purity of the final suspension is lower due to less than perfect efficiency. A summary showing the performance metrics and key features of these works was also given in Table 2.

4.1. Positive Separation

Positive separation of cells refers to the collection of a target cell population by a biomarker common to the population of interest. In terms of magnetophoresis, targets cells are often immunomagnetically labeled with magnetic beads and diverted from the rest of the blood sample. One recent work demonstrating this was performed by Shi et al. [70], where a smoothed herringbone structure offered grooves for capturing immunomagnetically labeled CTCs. Initially, magnetic particles conjugated with a CTC marker were trapped in the herringbone grooves with the external magnet. When the sample was introduced into the chip, the magnetic particles preferentially attached to the CTCs via antigen–antibody interaction. In addition, the work used the removal of the magnet for the release of the captured cells, and achieved a capture efficiency of 92% at 540 µL/h [70]. Similarly, Huang et al. [71] took a trapping approach, using a microwell array to confine individual cells and eliminate aggregation issues (Figure 7). This method achieved trapping of acute monocytic leukemia cells at an efficiency of 62% with a 99.6% purity. While

the microwells made the imaging and the quantification free from aggregates, the target biomarker in the study was a common antigen for leukocytes regardless of whether they are healthy or malignant.

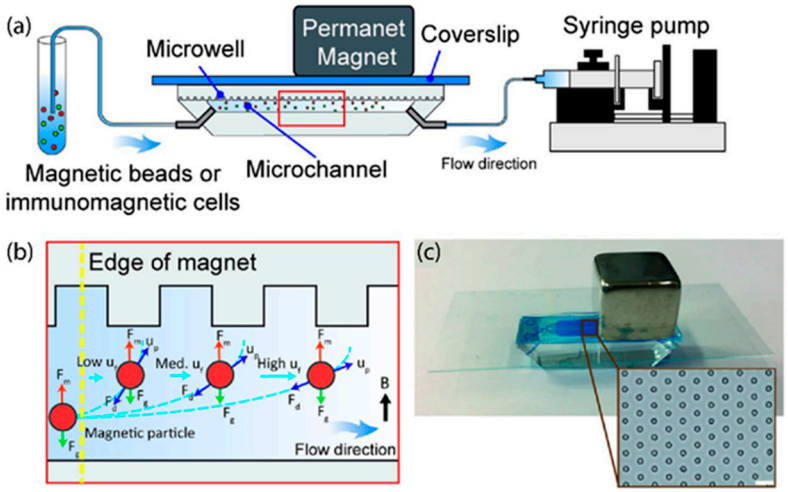

Figure 7. Magnetic trapping of individual cells in microwells. (**a**) Schematic of the system and its operation. (**b**) Illustration of the magnetic behavior of cells within the microfluidic chip. (**c**) Image of the device. The inset shows the microscopic image of the microwells. Scale bar represents 50 µm. Reproduced with permission [71]. Copyright 2021 Springer Nature.

Ferromagnetic features have been used to overcome the rapidly decreasing magnetic field gradient moving away from the field source. Cho et al. [72] used ferromagnetic microwires patterned on a glass substrate for lateral separation of CTCs from blood under a continuous flow. The substrate was also made to be re-usable to enable complex microfabrication processes without resorting to periodic fabrication. The polymer layer, however, was made to be disposable to avoid contamination of analytes. The resulting platform was reported to outperform the commercial products by two orders of magnitude in the purity of the isolated population (33.3% vs. 0.32%). However, one disadvantage of the platform was that the system efficiency would be affected by other required processes such as RBC lysis and washing. Earhart et al. [73], on the other hand, took a different approach and used a magnetic pore structure microfabricated by deposition of permalloy on a silicon substrate containing the pores. Unlike lateral flow systems where the fluid flows within the plane of microfluidic features, Earhart et al. [73] designed their system to operate like a conventional filter (Figure 8), in which the fluid flows normal to the plane of micropores. This approached allowed them to significantly improve throughput and to process samples at a rate as high as 25 mL per hour and reach 95.7% peak capture efficiency at 10 mL per hour [73].

4.2. Negative Separation

Negative separation in cancer cell applications target WBCs and their elimination. To selectively remove WBCs from the sample, the common WBC biomarkers such as CD15 [74], CD45 and CD66b are used [75], and various commercial magnetic beads already conjugated with these markers are available. This approach has the advantage of separating cancer cells with unknown biomarkers and leaving these cells untouched. However, it may not yield purities as high as positive enrichment. This stems from the fact that not all nucleated cells in normally present in blood can be completely depleted with a single or dual target antigen, for example endothelial progenitor cells do not express either CD45 or CD66b [76], but express CD31 [64,77].

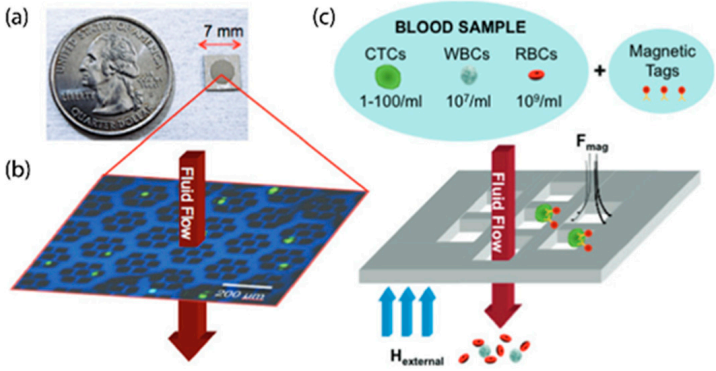

Figure 8. Magnetic cell sifter. (**a**) Image of the sifter. (**b**) Optical micrograph of the pore array and the trapped CTCs (green). (**c**) Operational principle. Immunomagnetically labeled CTCs are immobilized by the high magnetic gradient on the edges of the pores while other cells pass unaffected. Reproduced with permission [73]. Copyright 2021 RSC.

One of the most impactful displays of magnetic negative separation for CTCs was demonstrated by Karabacak et al. [78]. In their system, RBCs were first depleted by deterministic lateral displacement [74,79], then WBCs were sorted out using CD45 and CD66b conjugated magnetic particles from a focused fluidic stream into waste (Figure 9). The quadrupole magnet configuration enabled a two-step magnetophoresis. In the first step, high-expressing WBCs (large number of magnetic beads) were eliminated under a softer magnetic gradient, and the second step removed the lower expressors under a larger magnetic gradient with a total WBC removal efficiency of 99.9%. The overall system had the capability of processing large volumes of clinical samples to enrich sufficient number of CTCs for downstream analysis.

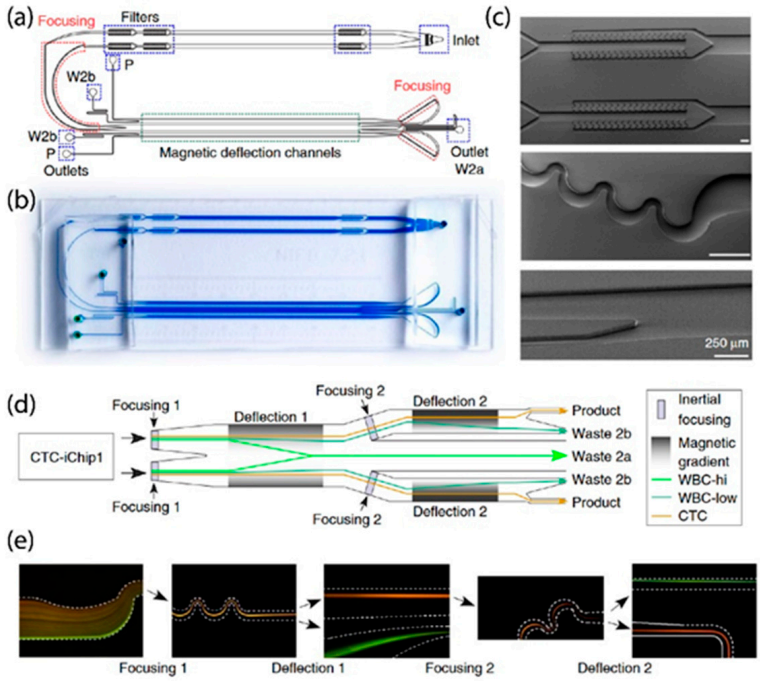

Figure 9. Design of the magnetophoretic module for CTC enrichment. (**a**) CAD design (**b**) Image of the microfluidic chip (**c**) Electron microscopy images showing the microfluidic filtration (top), inertial focusing (middle) and deflection channels (bottom). (**d**) Simplified operation of the magnetophoretic chip. (**e**) Fluorescent imaging of the microfluidic features while the device is in operation. Reproduced with permission [78]. Copyright 2014 Nature Publishing Group.

Sajay et al. [80–82] proposed a microfluidic chip with an immunomagnetic chamber coupled with a microslit membrane. WBCs were depleted by CD45-conjugated magnetic beads on their surface under a sandwich setup of permanent magnets. Then, CTCs were sifted with the microslit, while RBCs passed through the membrane. Based on the choice of trapping WBCs on the top and bottom surfaces of the microfluidic device, the chip had a fundamental limit of processing up to 2 mL blood samples due to the limited surface area [80]. Regardless, their magnetic trapping offered WBC depletion up to 99.93%. In a similar approach, Hyun et al. [83] depleted the WBCs labeled with CD45-conjugated magnetic beads with magnets sandwiching the microfluidic chip. The device was coupled with a downstream positive enrichment stage to further isolate the CTC selectively based on a cancer biomarker. However, processing large volumes of a sample remained a challenge due to the limited surface area. Moreover, the RBCs were lysed before the sample was introduced to the device, introducing potential loss of CTCs.

Lee et al. [84] developed an interesting system combining physical separation for RBCs and magnetophoretic separation for WBCs to acquire CTCs from blood samples. A slanted micro-weir [85] with a 7-micron gap between sides allowed RBCs to cross the weir while the rest of the cells were driven to the second module. In the magnetophoretic stage, WBCs carrying CD45 conjugated magnetic beads were diverted away from the main fluidic stream, and CTCs were isolated from blood.

Using a similar microwire structure to Byeon et al. [59] and Cho et al. [72], Kang et al. [86] established a negative separator for the purification of CTCs from blood. CD45- and CD66b-conjugated magnetic beads were used to tag WBCs in the sample. When the sample was introduced to the microfluidic device, unbound magnetic beads were first eliminated using ferromagnetic wires placed parallel to the fluid flow. In this region, magnetically labeled WBCs pass unaffected thanks to the larger drag forces due to their larger size. The WBCs were then eliminated from the primary stream by ferromagnetic wires [59,72,86] patterned on the substrate at an angle (Figure 10). The group also operated the device for positive enrichment of CTCs. Comparing the two approaches, they reported significantly lower CTC purity via negative depletion (~4–9%), which wouldn't be sufficient for a downstream analysis.

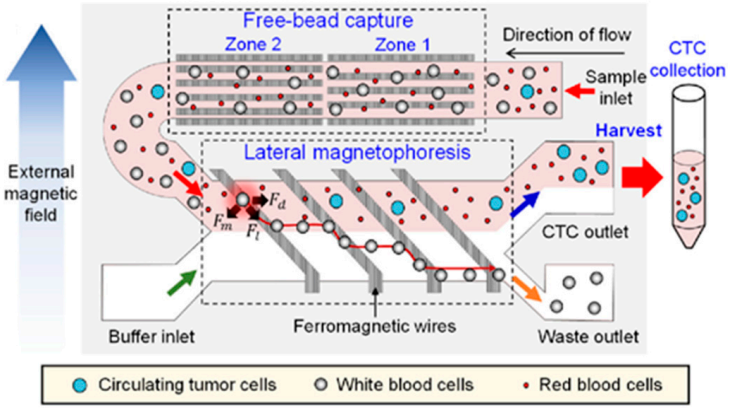

Figure 10. Negative enrichment of CTCs using ferromagnetic wires. In Zone 1 and Zone 2, unbound beads are eliminated from the rest of the sample due to low Drag forces on magnetic beads. Then, immunomagnetically labeled cells are removed from the main fluidic stream via ferromagnetic wires under external magnetic field. Reproduced with permission [86]. Copyright 2019 MDPI.

Table 2. Summary of the recent magnetophoretic positive and negative enrichment of CTCs.

Authors	Purpose	Target Biomarker	Key Feature	Metrics	Throughput
Shi et al. (2017) [70]	Positive isolation of CTCs	EpCAM (CD326)	Herringbone structure to create capture pockets	92% efficiency	0.54 mL/h
Huang et al. (2018) [71]	Positive isolation of leukemia cells	CD45	Immune to cell and bead aggregation	62% efficiency 99.6% purity	70 µL/min
Cho et al. (2017) [72]	Positive isolation of CTCs	EpCAM (CD326)	Reusable substrate with disposable fluidic layer	90% 33.3% purity	2 mL/h
Earhart et al. (2013) [73]	Positive isolation of CTCs	EpCAM (CD326)	Perpendicular flow enables higher processing speeds	95.7% 92.7% release efficiency	10 mL/h
Karabacak et al. (2014) [78]	WBC depletion for CTC enrichment	CD45, CD66b	Processing directly whole blood, integration with other microfluidic systems for clinical-grade use	99.9% WBC depletion97% CTC recovery	8 mL/h
Sajay et al. (2014) [82]	WBC depletion for CTC enrichment	CD45	Centrifugation-free, lysis-free approach	99.98% WBC depletion 80% CTC recovery	500 µL/min
Hyun et al. (2015) [83]	WBC depletion for CTC enrichment	CD45, EpCAM, HER2	Downstream positive enrichment of CTCs expressing a specific biomarker	99.9% WBC depletion	400 µL/min
Lee et al. (2020) [84]	WBC depletion for CTC enrichment	CD45	Integration with a slanted weir for physical filtration	97.2% WBC depletion93.3% purity	5 mL/h
Kang et al. (2019) [86]	WBC depletion, CTC isolation	CD45, CD66b, EpCAM	Direct comparison of negative and positive enrichment metrics	99.95% WBC depletion 83.1% CTC recovery 4-9% CTC purity	2.8 mL/h

5. Differential Sorting of Cells Using Magnetophoresis

Besides binary sorting, magnetophoresis is also used to differential analysis of samples, as summarized in Table 3. The differential approach can further be divided into two categories: differentiation of multiple markers in a single platform (i.e., multiplexing); and differentiation of a population at a single cell level to uncover population-level characteristics.

5.1. Multiplexed Sorting

One major downside of magnetic sorting is that the underlying mechanism is based on only a single parameter, which is magnetic susceptibility. Whether it is the hemoglobin content or a magnetic bead, separating populations based on multiple biomarkers in magnetophoresis remains challenging [41,87]. One platform addressing this limitation was shown by Adams et al. [88]. The microfluidic device (Figure 11) incorporated two arrays of ferromagnetic strips angled at 15° and 5° with respect to the fluidic flow. The sample was labeled with two different magnetic beads, more specifically 4.5 µm and 2.8 µm particles. The first sorting region with strips at a 15° angle generated enough transverse magnetic force on the cells with the larger magnetic beads to overcome the drag forces and guided them to the first outlet. Cells with the smaller magnetic beads, however, passed through this region unaffected as the drag forces were larger than the magnetic pull force. These cells were separated from the suspension in the second sorting region with longer ferromagnetic strips that are angled at 5°. The rest of the suspension was discarded through the waste outlet. The group also applied a similar technique to sort multiple bacterial targets from a mixed suspension by employing dielectrophoretic and magnetophoretic labels [89]. Although other works have demonstrated separations using different-sized magnetic beads for multiplexed sorting in microfluidics [90–92], the target population in these works were either beads or pathogens instead of cells.

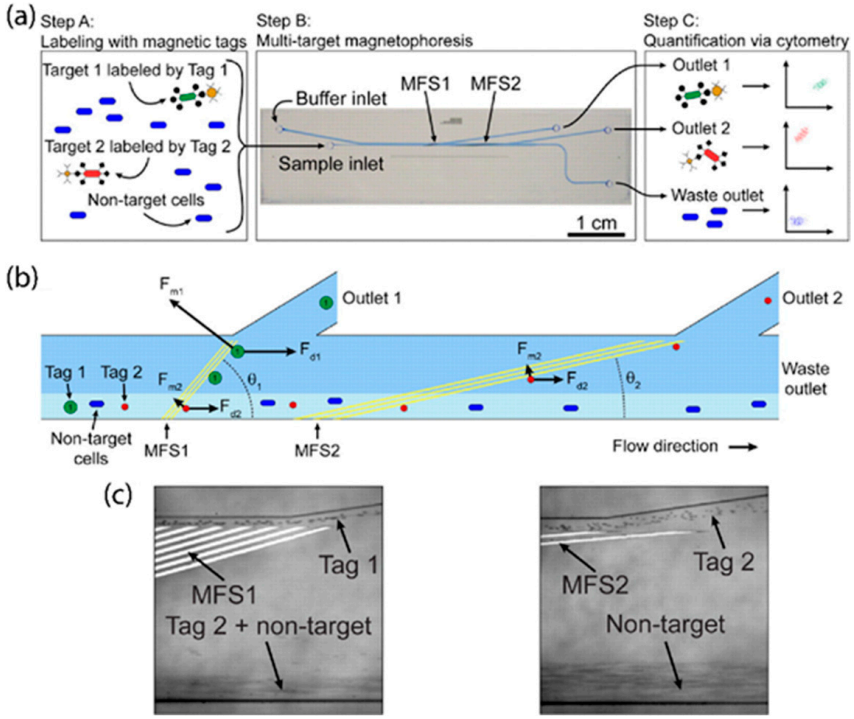

Figure 11. Multiplexed magnetophoretic sorting structure. (**a**) Operational summary of the device. (**b**) Illustration of the forces acting on the cells across the device. (**c**) Microscopic images of multiplexed sorting during operation. Reproduced with permission [88]. Copyright 2008 PNAS.

5.2. Population Level Measurements

Magnetically sorting the cell populations into distinct outlets and their consecutive quantification is a robust method to distinguish the single-cell-level traits in a cell population. This is often achieved with magnetically labeling the target cells as the magnetophoretic mobilities were shown to be a function of the expression of the targeted biomarker [93–95]. Based on this principle, Pamme et al. [96,97] investigated cell sorting based on the endocytosis of magnetic nanoparticles. Incubating the nanoparticles with various cell types, they demonstrated differential sorting of those cell populations based on the cell size and their magnetic susceptibility after nanoparticle uptake into different fluidic outlets under a magnetic field. The main limitation of their approach was that the quantification of the fractionated cells relied on optical video recordings.

Civelekoglu et al. [98], on the other hand, used differential sorting to profile a cell population based on the expression levels of a surface biomarker. In this work, immunomagnetically labeled cells were continuously deflected under an external magnetic field, and the cells in the outlets were quantified by multiplexed electrical sensors [99] as they were being sorted. Civelekoglu et al. [100,101] also demonstrated high-dynamic-range operation for their magnetophoretic system, with an interesting inspiration from digital photography. By modulating the flow rate during operation, they expanded their dynamic range to cover cases with high cell heterogeneity. Later, the group presented an integrated magnetophoretic sorter (Figure 12) with computational measurements to estimate the number of magnetic beads present on the surface of the cells from their sensor reading and made a direct comparison to conventional fluorescent measurements [102,103]. Furthermore, the group showed an integrated platform that coupled their differential sorting technique with an inline magnetic positive enrichment stage profile the surface markers in blood samples directly [104], a capability that commercial flow cytometers do not possess. They demonstrated up to 96% efficiency for their enrichment stage and an optimal processing speed of 1.5 mL/h with a throughput of up to 960 cells/s.

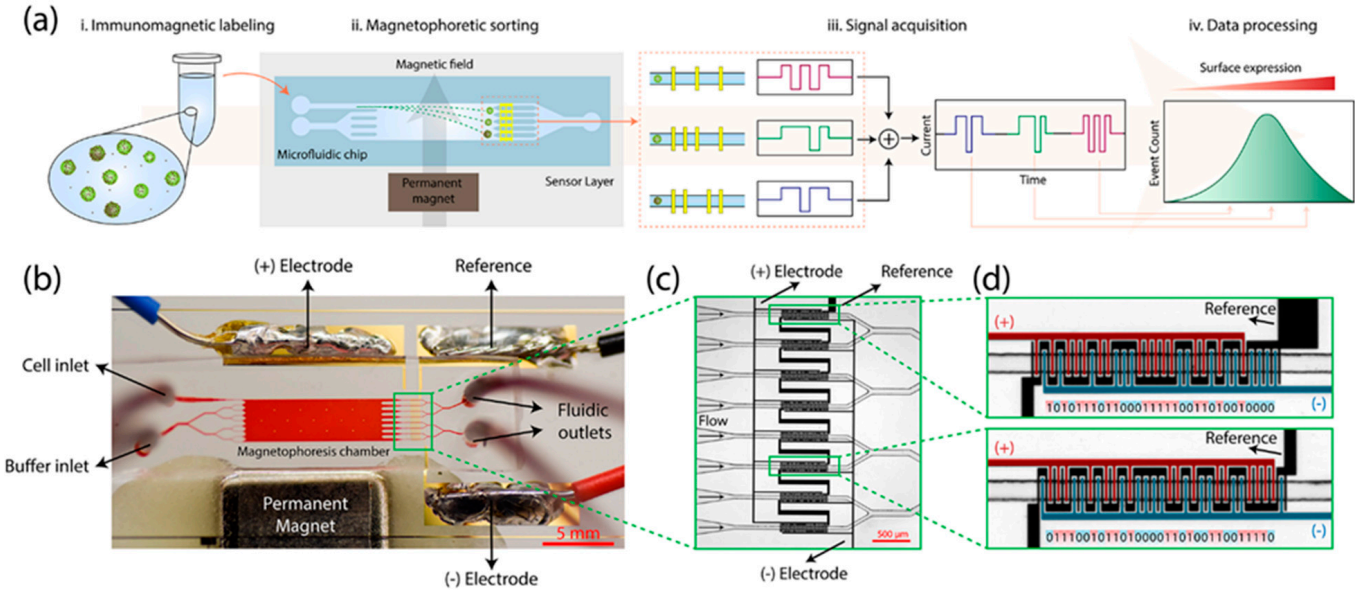

Figure 12. Magnetophoretic flow cytometer. (**a**) Operation principle. (**b**) Image of the microfluidic device. (**c**,**d**) Microscopy images of the electrical sensors for in-line quantification. Reproduced with permission [103]. Copyright 2019 RSC.

Similarly, Jack et al. [105] built a magnetophoretic sorter to separate cancer cells into three subpopulations based on their EpCAM expression (high, moderate, and low). In the initial stage, the high expressor population is collected via magnets placed 2.3 mm away from the microfluidic device. In the second stage, the magnets were placed 1.2 mm away for a larger gradient. The moderate expressors were collected from dedicated outlet, and the population passing unsorted from the second stage was considered as the low expressors. We should note that the platform was limited to only three levels of differentiation (low, medium, and high), and relied on optical recordings for the quantification of each subpopulation.

Using micropatterned ferromagnetic features on the device substrate, Poudineh et al. [106] and Labib et al. [107] developed a magnetophoretic ranking system to characterize the surface biomarker and intracellular protein expressions, respectively. The increasing size of the ferromagnetic features created a capture region differentially trapping cells based on their expression levels. High expressors were trapped earlier by even smaller features, while lower expressors could only be captured by the larger features present in the later sections of the chip. The quantification of the captured cells was performed by immunofluorescent scanning of the chip. O'Kelley's group demonstrated this technique to profile EpCAM expression of CTCs at a population level [106] and the intercellular proteins (Figure 13) of prostate cancer cells [107].

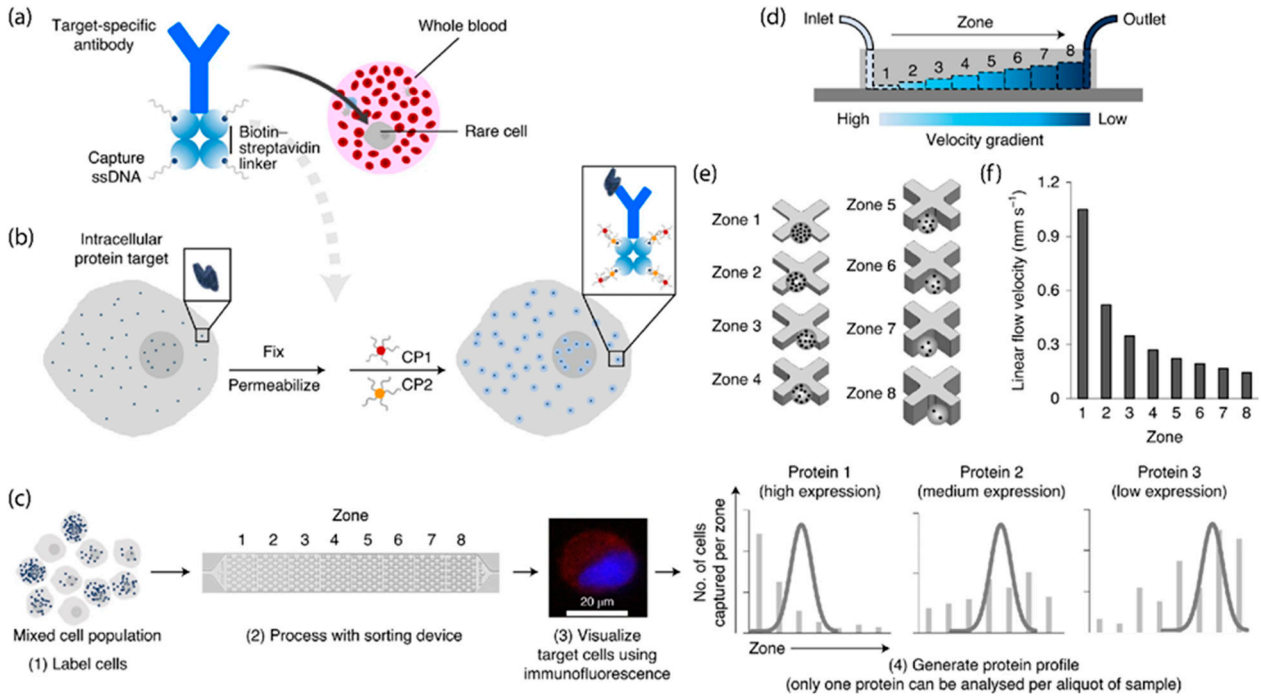

Figure 13. Magnetophoretic cell ranking based on the intercellular protein expression. (**a**) Labeling process. (**b**) Preparation of the cells for intercellular update. (**c**) Process flow. (**d**) Illustration of the vertical cross section of the device to selectively capture cells based on their different magnetic contents. (**e**) Visualization of the ferromagnetic features in each capture zone. (**f**) Average flow velocity in each capture zone. Reproduced with permission [107]. Copyright 2021 Nature Publishing Group.

6. Discussion

From its emergence to the present day, magnetic separation in microfluidic platforms has become a widely used technique to separate blood cells, purify rare cells, isolate CTCs, and characterize samples at a single-cell level thanks to its simplicity and high throughput. The separation of specific cells can be finely controlled by engineering the external magnetic field using neodymium permanent magnets or current-carrying wires, as well as patterning ferromagnetic features on the substrate to concentrate the magnetic flux wherever it is desired. Whether it is the native magnetic properties of a cell, invagination of magnetic nanoparticles, or functionalization of magnetic nano-/micro-beads with a specific surface marker, magnetophoresis consistently delivers high-efficiency sorting with great purity.

Besides the research domain, magnetic cell sorting has established a solid presence in the life sciences industry. Currently, there are multiple commercial product lines that are offered for magnetic cell sorting as ready-to-go kits, such as Dynabeads® (Invitrogen, Carlsbad, CA, USA), MACS® beads (Miltenyi Biotec, Auburn, CA, USA), EasySep® beads (STEMCELL Technologies, Vancouver, BC, Canada) or IMAG® beads (BD Biosciences, San Jose, CA, USA). The abundance of different bead sizes and pre-conjugated (or effortlessly conjugatable) variations has truly accelerated the developments of new microfluidic platforms. However, to date, one fundamental limitation of magnetic sorting still remains. Although multiplexing has been demonstrated in magnetic sorting at a population level, co-expression measurements still cannot be performed at a single-cell level. Currently, multi-color flow cytometry can measure dozens of biomarkers on a single cell using different fluorescent channels. In this sense, magnetic sorting behaves like a "monochrome" measurement that is incapable of differentiating one biomarker from another. Once this issue is resolved, we expect to see more and more microfluidic platforms targeting diagnostics and prognostics at the point of care.

Table 3. Summary of the recent magnetophoretic platforms for non-binary separations.

Authors	Purpose	Target Biomarker	Key Feature	Metrics	Throughput
Adams et al. (2008) [88]	Multitarget sorting of bacterial populations	T7 tag (4.5 µm bead), CPX-SA1 (2.8 µm bead)	Multiplexing magnetic sorting beyond binary separation	90%	10^9 cells/h
Robert et al. (2011) [96]	Differentiation of monocytes and macrophages based on nanoparticle uptake	Endocytosis of 8.7 nm iron oxide nanoparticles	Differential sorting into distinct outlets	88% purity 60% efficacy	10–100 cells/s
Civelekoglu et al. (2019) [103]	Profiling membrane expression in cell populations	EpCAM (CD326)	Differential sorting into distinct outlets, integrated electronic read-out	Used pre-purified suspension	500 cells/min
Civelekoglu et al. (2021) [104]	Profiling membrane expression directly from hematological samples	EpCAM (CD 326), CD45, CD34	Processing directly whole blood, integrated electronic read-out	85–96%	1.5 mL/h up to 960 cells/s
Jack et al. (2017) [105]	Non-binary sorting of cancer cells based on surface expression	EpCAM (CD326)	Fractionation can be controlled with the separation with of the magnets. Platform is limited to 3 levels of fractionation	Used pre-purified suspension	50 µL/min
Poudineh et al. (2016) [106]	Profiling membrane expression in cell populations	EpCAM, HER2, N-cadherin	Circular nickel micromagnets with increasing cross-section to differentially trap cells	92% cell recovery 98% cell viability	0.5 mL/h
Labib et al. (2020) [107]	Profiling intercellular proteins in rare cells	c-Myc, EpCAM, vimentin, PARP1, Oct4, POLRMT	Nickel features with increasing thickness to differential capture	~83% capture efficiency	2 mL/h

Overall, this review provides a brief history of how magnetic cell sorting was transitioned into microfluidic domain and demonstrates the evolution of magnetophoresis into numerous cell applications in recent years. This review specifically groups recent applications on the basis of the types of cells targeted for separation, and the growth of magnetophoresis beyond a simple binary sorting mechanism.

Author Contributions: Writing-original draft, O.C.; Writing-review and editing, O.C., A.B.F., A.F.S. All authors have read and agreed to the published version of the manuscript.

Funding: This work was supported by the National Science Foundation through ECCS 1610995 and ECCS 1752170 grants, and the Arnold and Mabel Beckman Foundation through Beckman Young Investigator Award to A.F.S.

Institutional Review Board Statement: Not applicable.

Informed Consent Statement: Not applicable.

Conflicts of Interest: The authors declare no conflict of interest.

References

1. Takayasu, M.; Duske, N.; Ash, S.; Friedlaender, F. HGMS studies of blood cell behavior in plasma. *IEEE Trans. Magn.* **1982**, *18*, 1520–1522. [CrossRef]
2. Kronick, P.; Gilpin, R.W. Use of superparamagnetic particles for isolation of cells. *J. Biochem. Biophys. Methods* **1986**, *12*, 73–80. [CrossRef]
3. Kantor, A.B.; Gibbons, I.; Miltenyi, S.; Schmitz, J. Magnetic cell sorting with colloidal superparamagnetic particles. *Cell Sep. Methods Appl.* **1998**, *1*, 153–173.
4. Grützkau, A.; Radbruch, A. Small but mighty: How the MACS®-technology based on nanosized superparamagnetic particles has helped to analyze the immune system within the last 20 years. *Cytom. Part A* **2010**, *77*, 643–647. [CrossRef] [PubMed]
5. Plouffe, B.; Murthy, S.K.; Lewis, L.H. Fundamentals and application of magnetic particles in cell isolation and enrichment: A review. *Rep. Prog. Phys.* **2014**, *78*, 016601. [CrossRef] [PubMed]
6. Olsvik, O.; Popovic, T.; Skjerve, E.; Cudjoe, K.S.; Hornes, E.; Ugelstad, J.; Uhlen, M. Magnetic separation techniques in diagnostic microbiology. *Clin. Microbiol. Rev.* **1994**, *7*, 43–54. [CrossRef]

7. Jing, Y.; Moore, L.R.; Williams, P.S.; Chalmers, J.J.; Farag, S.S.; Bolwell, B.; Zborowski, M. Blood progenitor cell separation from clinical leukapheresis product by magnetic nanoparticle binding and magnetophoresis. *Biotechnol. Bioeng.* **2007**, *96*, 1139–1154. [CrossRef]
8. Schumm, M.; Lang, P.; Taylor, G.; Kuci, S.; Klingebiel, T.; Buhring, H.J.; Handgretinger, R. Isolation of highly purified autologous and allogeneic peripheral CD34(+) cells using the CliniMACS device. *J. Hematotherapy* **1999**, *8*, 209–218. [CrossRef]
9. Wang, X.; Rivière, I. Clinical manufacturing of CAR T cells: Foundation of a promising therapy. *Mol. Ther. Oncolytics* **2016**, *3*, 16015. [CrossRef]
10. Lennartz, S.; Lock, D.; Kolbe, C.; Winkels, G.; Assenmacher, M.; Kaiser, A. StraightFrom®MicroBeads: Fast T cell isolation for CAR T cell manufacturing without density gradient centrifugation. *J. Immunol.* **2020**, *204* (Suppl. S1), 86.28.
11. Ziarati, N.; Tavalaee, M.; Bahadorani, M.; Esfahani, M.H.N. Clinical outcomes of magnetic activated sperm sorting in infertile men candidate for ICSI. *Hum. Fertil.* **2018**, *22*, 118–125. [CrossRef]
12. Dirican, E.K.; Özgün, O.D.; Akarsu, S.; Akın, K.O.; Ercan, O.; Uğurlu, M.; Çamsarı, Ç.; Kanyılmaz, O.; Kaya, A.; Ünsal, A. Clinical outcome of magnetic activated cell sorting of non-apoptotic spermatozoa before density gradient centrifugation for assisted reproduction. *J. Assist. Reprod. Genet.* **2008**, *25*, 375–381. [CrossRef]
13. Bonner, W.A.; Hulett, H.R.; Sweet, R.G.; Herzenberg, L.A. Fluorescence Activated Cell Sorting. *Rev. Sci. Instrum.* **1972**, *43*, 404–409. [CrossRef] [PubMed]
14. Melville, D.; Paul, F.; Roath, S. Direct magnetic separation of red cells from whole blood. *Nature* **1975**, *255*, 706. [CrossRef]
15. Haik, Y.; Pai, V.; Chen, C.-J. Development of magnetic device for cell separation. *J. Magn. Magn. Mater.* **1999**, *194*, 254–261. [CrossRef]
16. Owen, C. High gradient magnetic separation of erythrocytes. *Biophys. J.* **1978**, *22*, 171–178. [CrossRef]
17. Takayasu, M.; Kelland, D.R.; Minervini, J. Continuous magnetic separation of blood components from whole blood. *IEEE Trans. Appl. Supercond.* **2000**, *10*, 927–930. [CrossRef]
18. Melville, D.; Paul, F.; Roath, S. Fractionation of blood components using high gradient magnetic separation. *IEEE Trans. Magn.* **1982**, *18*, 1680–1685. [CrossRef]
19. Owen, C.S. Magnetic sorting of leukocytes. *Cell Biophys.* **1986**, *8*, 287–296. [CrossRef]
20. Owen, C.; Lindsay, J. Ferritin as a label for high-gradient magnetic separation. *Biophys. J.* **1983**, *42*, 145–150. [CrossRef]
21. Owen, C.S.; Moore, E. High gradient magnetic separation of rosette-forming cells. *Cell Biophys.* **1981**, *3*, 141–153. [CrossRef]
22. Gerber, R. Magnetic filtration of ultra-fine particles. *IEEE Trans. Magn.* **1984**, *20*, 1159–1164. [CrossRef]
23. Senftle, F.E.; Hambright, W.P. Magnetic Susceptibility of Biological Materials. In *Biological Effects of Magnetic Fields*; Barnothy, M.F., Ed.; Springer: Boston, MA, USA, 1995; Volume 2, pp. 261–306.
24. Rios, A.; Escarpa, A.; Simonet, B. *Miniaturization of Analytical Systems*; John Wiley & Sons: Totowa, NJ, USA, 2009. [CrossRef]
25. Rios, A.; Escarpa, A.; Simonet, B. *Tools for the Design of Miniaturized Analytical Systems*; John Wiley & Sons: Totowa, NJ, USA, 2009; pp. 39–92. [CrossRef]
26. Voldman, J.; Gray, M.L.; Schmidt, M.A. Microfabrication in Biology and Medicine. *Annu. Rev. Biomed. Eng.* **1999**, *1*, 401–425. [CrossRef]
27. Tsao, C.-W. Polymer Microfluidics: Simple, Low-Cost Fabrication Process Bridging Academic Lab Research to Commercialized Production. *Micromachines* **2016**, *7*, 225. [CrossRef]
28. Rios, A.; Escarpa, A.; Simonet, B. *Portability of Miniaturized Analytical Systems*; John Wiley & Sons: Totowa, NJ, USA, 2009; pp. 345–355. [CrossRef]
29. Adams, J.D.; Soh, H.T. Perspectives on Utilizing Unique Features of Microfluidics Technology for Particle and Cell Sorting. *J. Lab. Autom.* **2009**, *14*, 331–340. [CrossRef]
30. Kumar, S.; Kumar, S.; Ali, A.; Anand, P.; Agrawal, V.V.; John, R.; Maji, S.; Malhotra, B.D. Microfluidic-integrated biosensors: Prospects for point-of-care diagnostics. *Biotechnol. J.* **2013**, *8*, 1267–1279. [CrossRef]
31. Du, G.; Fang, Q.; den Toonder, J.M.J. Microfluidics for cell-based high throughput screening platforms—A review. *Anal. Chim. Acta* **2016**, *903*, 36–50. [CrossRef]
32. Song, K.; Li, G.; Zu, X.; Du, Z.; Liu, L.; Hu, Z. The Fabrication and Application Mechanism of Microfluidic Systems for High Throughput Biomedical Screening: A Review. *Micromachines* **2020**, *11*, 297. [CrossRef] [PubMed]
33. Kant, K.; Shahbazi, M.-A.; Dave, V.P.; Ngo, T.A.; Chidambara, V.A.; Than, L.Q.; Bang, D.D.; Wolff, A. Microfluidic devices for sample preparation and rapid detection of foodborne pathogens. *Biotechnol. Adv.* **2018**, *36*, 1003–1024. [CrossRef] [PubMed]
34. Hung, L.-Y.; Chang, J.-C.; Tsai, Y.-C.; Huang, C.-C.; Chang, C.-P.; Yeh, C.-S.; Lee, G.-B. Magnetic nanoparticle-based immunoassay for rapid detection of influenza infections by using an integrated microfluidic system. *Nanomed. Nanotechnol. Biol. Med.* **2013**, *10*, 819–829. [CrossRef] [PubMed]
35. Wang, C.-H.; Lien, K.-Y.; Wu, J.-J.; Lee, G.-B. A magnetic bead-based assay for the rapid detection of methicillin-resistant Staphylococcus aureus by using a microfluidic system with integrated loop-mediated isothermal amplification. *Lab Chip* **2011**, *11*, 1521–1531. [CrossRef]
36. Jung, W.; Han, J.; Choi, J.-W.; Ahn, C.H. Point-of-care testing (POCT) diagnostic systems using microfluidic lab-on-a-chip technologies. *Microelectron. Eng.* **2015**, *132*, 46–57. [CrossRef]
37. Pandey, C.M.; Augustine, S.; Kumar, S.; Kumar, S.; Nara, S.; Srivastava, S.; Malhotra, B.D. Microfluidics Based Point-of-Care Diagnostics. *Biotechnol. J.* **2017**, *13*. [CrossRef]

38. Farahinia, A.; Zhang, W.; Badea, I. Novel microfluidic approaches to circulating tumor cell separation and sorting of blood cells: A review. *J. Sci. Adv. Mater. Devices* **2021**, *6*, 303–320. [CrossRef]
39. Surendran, A.N.; Zhou, R.; Lin, Y. Microfluidic Devices for Magnetic Separation of Biological Particles: A Review. *J. Med Devices* **2020**, *15*. [CrossRef]
40. Watarai, H.; Suwa, M.; Iiguni, Y. Magnetophoresis and electromagnetophoresis of microparticles in liquids. *Anal. Bioanal. Chem.* **2004**, *378*, 1693–1699. [CrossRef] [PubMed]
41. Pamme, N.; Manz, A. On-Chip Free-Flow Magnetophoresis: Continuous Flow Separation of Magnetic Particles and Agglomerates. *Anal. Chem.* **2004**, *76*, 7250–7256. [CrossRef]
42. Gijs, M.A.M. Magnetic bead handling on-chip: New opportunities for analytical applications. *Microfluid. Nanofluidics* **2004**, *1*, 22–40. [CrossRef]
43. Berger, M.; Castelino, J.; Huang, R.; Shah, M.; Austin, R.H. Design of a microfabricated magnetic cell separator. *Electrophoresis* **2001**, *22*, 3883–3892. [CrossRef]
44. Han, K.-H.; Frazier, A.B. Continuous magnetophoretic separation of blood cells in microdevice format. *J. Appl. Phys.* **2004**, *96*, 5797–5802. [CrossRef]
45. Ki-Ho, H.; Landers, J.P.; Frazier, A.B. Continuous paramagnetophoretic microseparator for blood cells in TRANSDUCERS '03. In Proceedings of the 12th International Conference on Solid-State Sensors, Actuators and Microsystems. Digest of Technical Papers (Cat. No. 03TH8664), Boston, MA, USA, 8–12 June 2003; Volume 2, pp. 1229–1232. [CrossRef]
46. Han, K.-H.; Frazier, A. Diamagnetic capture mode magnetophoretic microseparator for blood cells. *J. Microelectromech. Syst.* **2005**, *14*, 1422–1431. [CrossRef]
47. Han, K.-H.; Frazier, A.B. Paramagnetic capture mode magnetophoretic microseparator for high efficiency blood cell separations. *Lab Chip* **2005**, *6*, 265–273. [CrossRef]
48. Han, K.-H.; Frazier, A. Paramagnetic capture mode magnetophoretic microseparator for blood cells. *IEE Proc. Nanobiotechnol.* **2006**, *153*, 67–73. [CrossRef] [PubMed]
49. Inglis, D.; Riehn, R.; Austin, R.H.; Sturm, J.C. Continuous microfluidic immunomagnetic cell separation. *Appl. Phys. Lett.* **2004**, *85*, 5093–5095. [CrossRef]
50. Miltenyi, S.; Muller, W.; Weichel, W.; Radbruch, A. High gradient magnetic cell separation with MACS. *Cytometry* **1990**, *11*, 231–238. [CrossRef] [PubMed]
51. Furdui, V.I.; Harrison, D.J. Immunomagnetic T cell capture from blood for PCR analysis using microfluidic systems. *Lab Chip* **2004**, *4*, 614–618. [CrossRef]
52. Han, K.-H.; Han, A.; Frazier, A.B. Microsystems for isolation and electrophysiological analysis of breast cancer cells from blood. *Biosens. Bioelectron.* **2006**, *21*, 1907–1914. [CrossRef]
53. Kim, S.; Song, H.; Ahn, H.; Kim, T.; Jung, J.; Cho, S.K.; Shin, D.-M.; Choi, J.-R.; Hwang, Y.-H.; Kim, K. A Review of Advanced Impedance Biosensors with Microfluidic Chips for Single-Cell Analysis. *Biosensors* **2021**, *11*, 412. [CrossRef] [PubMed]
54. Shiriny, A.; Bayareh, M. On magnetophoretic separation of blood cells using Halbach array of magnets. *Meccanica* **2020**, *55*, 1903–1916. [CrossRef]
55. Halbach, K. Design of permanent multipole magnets with oriented rare earth cobalt material. *Nucl. Instrum. Methods* **1980**, *169*, 1–10. [CrossRef]
56. Descamps, L.; Audry, M.-C.; Howard, J.; Mekkaoui, S.; Albin, C.; Barthelemy, D.; Payen, L.; Garcia, J.; Laurenceau, E.; Le Roy, D.; et al. Self-Assembled Permanent Micro-Magnets in a Polymer-Based Microfluidic Device for Magnetic Cell Sorting. *Cells* **2021**, *10*, 1734. [CrossRef] [PubMed]
57. Verpoorte, E. Microfluidic chips for clinical and forensic analysis. *Electrophoresis* **2002**, *23*, 677–712. [CrossRef]
58. Yu, Z.T.F.; Yong, K.M.A.; Fu, J. Microfluidic Blood Cell Sorting: Now and Beyond. *Small* **2014**, *10*, 1687–1703. [CrossRef]
59. Byeon, Y.; Ki, C.-S.; Han, K.-H. Isolation of nucleated red blood cells in maternal blood for Non-invasive prenatal diagnosis. *Biomed. Microdevices* **2015**, *17*, 1–7. [CrossRef]
60. Hackett, S.; Hamzah, J.; Davis, T.; Pierre, T.S. Magnetic susceptibility of iron in malaria-infected red blood cells. *Biochim. Biophys. Acta BBA Mol. Basis Dis.* **2009**, *1792*, 93–99. [CrossRef] [PubMed]
61. Kim, J.; Massoudi, M.; Antaki, J.F.; Gandini, A. Removal of malaria-infected red blood cells using magnetic cell separators: A computational study. *Appl. Math. Comput.* **2012**, *218*, 6841–6850. [CrossRef]
62. Martin, A.B.; Wu, W.-T.; Kameneva, M.V.; Antaki, J.F. Development of a High-Throughput Magnetic Separation Device for Malaria-Infected Erythrocytes. *Ann. Biomed. Eng.* **2017**, *45*, 2888–2898. [CrossRef]
63. Glynn, M.T.; Kinahan, D.J.; Ducrée, J. Rapid, low-cost and instrument-free CD4+ cell counting for HIV diagnostics in resource-poor settings. *Lab Chip* **2014**, *14*, 2844–2851. [CrossRef] [PubMed]
64. Naeim, F.; Nagesh, R.P.; Song, S.X.; Phan, R.T. Chapter 2—Principles of Immunophenotyping. In *Atlas of Hematopathology*, 2nd ed.; Naeim, F., Nagesh, R.P., Song, S.X., Phan, R.T., Eds.; Academic Press: Cambridge, MA, USA, 2018; pp. 29–56.
65. Liu, Q.; Chernish, A.; DuVall, J.A.; Ouyang, Y.; Li, J.; Qian, Q.; Bazydlo, L.A.L.; Haverstick, D.M.; Landers, J.P. The ARTμS: A novel microfluidic CD4+ T-cell enumeration system for monitoring antiretroviral therapy in HIV patients. *Lab Chip* **2015**, *16*, 506–514. [CrossRef]
66. World Health Organization. *What's New in Treatment Monitoring: Viral Load and CD4 Testing*; Update; WHO: Geneva, Switzerland, 2017.

67. Wang, Z.; Sargent, E.H.; Kelley, S.O. Ultrasensitive Detection and Depletion of Rare Leukemic B Cells in T Cell Populations via Immunomagnetic Cell Ranking. *Anal. Chem.* **2021**, *93*, 2327–2335. [CrossRef]
68. Schneider, T.; Karl, S.; Moore, L.R.; Chalmers, J.J.; Williams, P.; Zborowski, M. Sequential CD34 cell fractionation by magnetophoresis in a magnetic dipole flow sorter. *Analyst* **2009**, *135*, 62–70. [CrossRef]
69. Plouffe, B.D.; Mahalanabis, M.; Lewis, L.H.; Klapperich, C.M.; Murthy, S.K. Clinically Relevant Microfluidic Magnetophoretic Isolation of Rare-Cell Populations for Diagnostic and Therapeutic Monitoring Applications. *Anal. Chem.* **2012**, *84*, 1336–1344. [CrossRef]
70. Shi, W.; Wang, S.; Maarouf, A.; Uhl, C.G.; He, R.; Yunus, D.; Liu, Y. Magnetic particles assisted capture and release of rare circulating tumor cells using wavy-herringbone structured microfluidic devices. *Lab Chip* **2017**, *17*, 3291–3299. [CrossRef]
71. Huang, N.-T.; Hwong, Y.-J.; Lai, R.L. A microfluidic microwell device for immunomagnetic single-cell trapping. *Microfluid. Nanofluidics* **2018**, *22*, 16. [CrossRef]
72. Cho, H.; Kim, J.; Jeon, C.-W.; Han, K.-H. A disposable microfluidic device with a reusable magnetophoretic functional substrate for isolation of circulating tumor cells. *Lab Chip* **2017**, *17*, 4113–4123. [CrossRef]
73. Earhart, C.M.; Hughes, C.E.; Gaster, R.S.; Ooi, C.C.; Wilson, R.J.; Zhou, L.Y.; Humke, E.W.; Xu, L.; Wong, D.J.; Willingham, S.B.; et al. Isolation and mutational analysis of circulating tumor cells from lung cancer patients with magnetic sifters and biochips. *Lab Chip* **2013**, *14*, 78–88. [CrossRef]
74. Ozkumur, E.; Shah, A.M.; Ciciliano, J.C.; Emmink, B.L.; Miyamoto, D.T.; Brachtel, E.; Yu, M.; Chen, P.-I.; Morgan, B.; Trautwein, J.; et al. Inertial Focusing for Tumor Antigen–Dependent and –Independent Sorting of Rare Circulating Tumor Cells. *Sci. Transl. Med.* **2013**, *5*, 179ra47. [CrossRef] [PubMed]
75. Van Der Toom, E.E.; Verdone, J.E.; Gorin, M.A.; Pienta, K.J. Technical challenges in the isolation and analysis of circulating tumor cells. *Oncotarget* **2016**, *7*, 62754–62766. [CrossRef] [PubMed]
76. Masouleh, B.K.; Baraniskin, A.; Schmiegel, W.; Schroers, R. Quantification of circulating endothelial progenitor cells in human peripheral blood: Establishing a reliable flow cytometry protocol. *J. Immunol. Methods* **2010**, *357*, 38–42. [CrossRef]
77. Yang, H.-M.; Kim, J.-Y.; Cho, H.-J.; Lee, J.-E.; Jin, S.; Hur, J.; Kwon, Y.-W.; Seong, M.-W.; Choi, E.-K.; Lee, H.-Y.; et al. NFATc1+CD31+CD45−Circulating multipotent stem cells derived from human endocardium and their therapeutic potential. *Biomaterials* **2019**, *232*, 119674. [CrossRef]
78. Karabacak, N.M.; Spuhler, P.S.; Fachin, F.; Lim, E.J.; Pai, V.; Ozkumur, E.; Martel, J.M.; Kojic, N.; Smith, K.; Chen, P.-I.; et al. Microfluidic, marker-free isolation of circulating tumor cells from blood samples. *Nat. Protoc.* **2014**, *9*, 694–710. [CrossRef]
79. McGrath, J.; Jimenez, M.; Bridle, H. Deterministic lateral displacement for particle separation: A review. *Lab Chip* **2014**, *14*, 4139–4158. [CrossRef]
80. Gourikutty, S.B.N.; Chang, C.-P.; Poenar, D.P. An integrated on-chip platform for negative enrichment of tumour cells. *J. Chromatogr. B* **2016**, *1028*, 153–164. [CrossRef]
81. Gourikutty, S.B.N.; Chang, C.-P.; Puiu, P.D. Microfluidic immunomagnetic cell separation from whole blood. *J. Chromatogr. B* **2016**, *1011*, 77–88. [CrossRef]
82. Sajay, B.N.G.; Chang, C.-P.; Ahmad, H.; Khuntontong, P.; Wong, C.C.; Wang, Z.; Puiu, P.D.; Soo, R.; Rahman, A.R.A. Microfluidic platform for negative enrichment of circulating tumor cells. *Biomed. Microdevices* **2014**, *16*, 537–548. [CrossRef]
83. Hyun, K.-A.; Lee, T.Y.; Lee, S.H.; Jung, H.-I. Two-stage microfluidic chip for selective isolation of circulating tumor cells (CTCs). *Biosens. Bioelectron.* **2015**, *67*, 86–92. [CrossRef] [PubMed]
84. Lee, J.; Sul, O.; Lee, S.-B. Enrichment of Circulating Tumor Cells from Whole Blood Using a Microfluidic Device for Sequential Physical and Magnetophoretic Separations. *Micromachines* **2020**, *11*, 481. [CrossRef]
85. Yoon, Y.; Lee, J.; Ra, M.; Gwon, H.; Lee, S.; Kim, M.Y.; Yoo, K.-C.; Sul, O.; Kim, C.G.; Kim, W.-Y.; et al. Continuous Separation of Circulating Tumor Cells from Whole Blood Using a Slanted Weir Microfluidic Device. *Cancers* **2019**, *11*, 200. [CrossRef]
86. Kang, H.; Kim, J.; Cho, H.; Han, K.-H. Evaluation of Positive and Negative Methods for Isolation of Circulating Tumor Cells by Lateral Magnetophoresis. *Micromachines* **2019**, *10*, 386. [CrossRef] [PubMed]
87. Yellen, B.B.; Erb, R.M.; Son, H.S.; Hewlin, J.R.; Shang, H.; Lee, G.U. Traveling wave magnetophoresis for high resolution chip based separations. *Lab Chip* **2007**, *7*, 1681–1688. [CrossRef] [PubMed]
88. Adams, J.D.; Kim, U.; Soh, H.T. Multitarget magnetic activated cell sorter. *Proc. Natl. Acad. Sci. USA* **2008**, *105*, 18165–18170. [CrossRef] [PubMed]
89. Kim, U.; Soh, H.T. Simultaneous sorting of multiple bacterial targets using integrated Dielectrophoretic–Magnetic Activated Cell Sorter. *Lab Chip* **2009**, *9*, 2313–2318. [CrossRef]
90. Kumar, V.; Rezai, P. Multiplex Inertio-Magnetic Fractionation (MIMF) of magnetic and non-magnetic microparticles in a microfluidic device. *Microfluid. Nanofluidics* **2017**, *21*, 83. [CrossRef]
91. Khashan, S.A.; Dagher, S.; Alazzam, A. Microfluidic multi-target sorting by magnetic repulsion. *Microfluid. Nanofluidics* **2018**, *22*, 64. [CrossRef]
92. Ngamsom, B.; Esfahani, M.M.N.; Phurimsak, C.; Lopez-Martinez, M.J.; Raymond, J.-C.; Broyer, P.; Patel, P.; Pamme, N. Multiplex sorting of foodborne pathogens by on-chip free-flow magnetophoresis. *Anal. Chim. Acta* **2016**, *918*, 69–76. [CrossRef] [PubMed]
93. McCloskey, K.E.; Chalmers, J.J.; Zborowski, M. Magnetic Cell Separation: Characterization of Magnetophoretic Mobility. *Anal. Chem.* **2003**, *75*, 6868–6874. [CrossRef]

94. McCloskey, K.; Moore, L.; Hoyos, M.; Rodriguez, A.; Chalmers, J.; Zborowski, M. Magnetophoretic Cell Sorting Is a Function of Antibody Binding Capacity. *Biotechnol. Prog.* **2003**, *19*, 899–907. [CrossRef] [PubMed]
95. McCloskey, K.E.; Chalmers, J.J.; Zborowski, M. Magnetophoretic mobilities correlate to antibody binding capacities. *Cytometry* **2000**, *40*, 307–315. [CrossRef]
96. Robert, D.; Pamme, N.; Conjeaud, H.; Gazeau, F.; Iles, A.; Wilhelm, C. Cell sorting by endocytotic capacity in a microfluidic magnetophoresis device. *Lab Chip* **2011**, *11*, 1902–1910. [CrossRef]
97. Pamme, N.; Wilhelm, C. Continuous sorting of magnetic cells via on-chip free-flow magnetophoresis. *Lab Chip* **2006**, *6*, 974–980. [CrossRef]
98. Civelekoglu, O.; Liu, R.; Boya, M.; Chu, C.-H.; Wang, N.; Sarioglu, A.F. A microfluidic device for electronic cell surface expression profiling using magnetophoresis. In Proceedings of the 2017 19th International Conference on Solid-State Sensors, Actuators and Microsystems (TRANSDUCERS), Kaohsiung, Taiwan, 18–22 June 2017; pp. 480–483. [CrossRef]
99. Liu, R.; Wang, N.; Kamili, F.; Sarioglu, A.F. Microfluidic CODES: A scalable multiplexed electronic sensor for orthogonal detection of particles in microfluidic channels. *Lab Chip* **2016**, *16*, 1350–1357. [CrossRef] [PubMed]
100. Civelekoglu, O.; Wang, N.; Boya, M.; Ozkaya-Ahmadov, T.; Liu, R.; Sarioglu, A.F. High Dynamic Range Electrical Profiling of Surface Expression via Flow-Rate-Modulated-Magnetophoresis. In Proceedings of the 22nd International Conference on Miniaturized Systems for Chemistry and Life Sciences, Kaohsiung, Taiwan, 11–15 November 2018.
101. Civelekoglu, O.; Wang, N.; Boya, M.; Ozkaya-Ahmadov, T.; Liu, R.; Sarioglu, A.F. Digital Photography Techniques in Microfluidics: Exposure Bracketing for High Dynamic Range Magnetophoretic Cytometry. In Proceedings of the 23rd International Conference on Miniaturized Systems for Chemistry and Life Sciences, Basel, Switzerland, 27–31 October 2019.
102. Civelekoglu, O.; Wang, N.; Boya, M.; Ozkaya-Ahmadov, T.; Liu, R.; Sarioglu, A.F. Quantitative Measurement of Cell Surface Expression Via Magnetophoretic Cytometry. In Proceedings of the 20th International Conference on Solid-State Sensors, Actuators and Microsystems & Eurosensors XXXIII (TRANSDUCERS & EUROSENSORS XXXIII), Berlin, Germany, 23–27 June 2019; pp. 975–978. [CrossRef]
103. Civelekoglu, O.; Wang, N.; Boya, M.; Ozkaya-Ahmadov, T.; Liu, R.; Sarioglu, A.F. Electronic profiling of membrane antigen expressionviaimmunomagnetic cell manipulation. *Lab Chip* **2019**, *19*, 2444–2455. [CrossRef]
104. Civelekoglu, O.; Liu, R.; Usanmaz, C.F.; Chu, C.-H.; Boya, M.; Ozkaya-Ahmadov, T.; Arifuzzman, A.K.M.; Wang, N.; Sarioglu, A.F. Electronic Measurement of Cell Antigen Expression in Whole Blood. *Lab Chip* **2021**. [CrossRef] [PubMed]
105. Jack, R.; Hussain, K.; Rodrigues, D.; Zeinali, M.; Azizi, E.; Wicha, M.; Simeone, D.M.; Nagrath, S. Microfluidic continuum sorting of sub-populations of tumor cells via surface antibody expression levels. *Lab Chip* **2017**, *17*, 1349–1358. [CrossRef] [PubMed]
106. Poudineh, M.; Aldridge, P.M.; Ahmed, S.; Green, B.J.; Kermanshah, L.; Nguyen, V.; Tu, C.; Mohamadi, R.M.; Nam, R.K.; Hansen, A.; et al. Tracking the dynamics of circulating tumour cell phenotypes using nanoparticle-mediated magnetic ranking. *Nat. Nanotechnol.* **2016**, *12*, 274–281. [CrossRef]
107. Labib, M.; Wang, Z.; Ahmed, S.U.; Mohamadi, R.M.; Duong, B.; Green, B.; Sargent, E.H.; Kelley, S.O. Tracking the expression of therapeutic protein targets in rare cells by antibody-mediated nanoparticle labelling and magnetic sorting. *Nat. Biomed. Eng.* **2020**, *5*, 41–52. [CrossRef]